WCAP 10576

TECHNICAL BASIS FOR ELIMINATING THE RHR LINE RUPTURE AS THE STRUCTURAL DESIGN BASIS FOR CATAWBA UNITS 1 AND 2 AND MCGUIRE UNITS 1 AND 2

S. A. Swamy
J. C. Schmertz
R. A. Holmes
C. Y. Wang
Y. S. Lee

June 1984

APPROVED: _____
J. N. Chirigos, Manager
Structural Materials
Engineering

APPROVED: _____
E. R. Johnson, Manager
Structural and Seismic
Development

Work performed under Shop Order DXNJ 950

WESTINGHOUSE ELECTRIC CORPORATION

Nuclear Energy Systems
P.O. Box 355
Pittsburgh, Pennsylvania 15230

FOREWORD

This document contains Westinghouse Electric Corporation proprietary information and data which has been identified by brackets. Coding associated with the brackets set forth the basis on which the information is considered proprietary. These codes are listed with their meanings in WCAP-7211.

The proprietary information and data contained in this report were obtained at considerable Westinghouse expense and its release could seriously affect our competitive position. This information is to be withheld from public disclosure in accordance with the Rules of Practice, 10 CFR 2.790 and the information presented herein be safeguarded in accordance with 10 CFR 2.903. Withholding of this information does not adversely affect the public interest.

This information has been provided for your internal use only and should not be released to persons or organizations outside the Directorate of Regulation and the ACRS without the express written approval of Westinghouse Electric Corporation. Should it become necessary to release this information to such persons as part of the review procedure, please contact Westinghouse Electric Corporation, which will make the necessary arrangements required to protect the Corporation's proprietary interests.

The proprietary information is deleted in the unclassified version of this report.

TABLE OF CONTENTS

TABLE OF CONTENTS (Cont'd)

LIST OF FIGURES

LIST OF FIGURES

LIST OF TABLES

1.0 INTRODUCTION

1.1 BACKGROUND

The current structural design basis for the Residual Heat Removal (RHR) line requires postulating non-mechanistic circumferential (guillotine) breaks in which the pipe is assumed to rupture along the full circumference of the pipe. This results in overly conservative estimates of support loads. It is, therefore, highly desirable to be realistic in the postulation of pipe breaks for the RHR line. Presented in this report are the descriptions of a mechanistic pipe break evaluation method and the analytical results that can be used for establishing that a guillotine type break will not occur within the portion of RHR line between the hot leg and the first isolation valve. The evaluations considering circumferentially oriented flaws cover longitudinal cases.

1.2 SCOPE AND OBJECTIVE

The general purpose of this investigation is to show that a circumferential flaw which is larger than any flaw that would be present in the RHR line will remain stable when subjected to the worst combination of plant loadings. The flaw stability criteria proposed for the analysis will examine both the global and local stability. The global analysis is carried out using the [+a,c,e]+ method, based on traditional [ ]+ concepts, +a,c,e but accounting for [ ]+ and taking into account the presence +a,c,e of a flaw. This analysis using faulted loading conditions enables determination of the critical flaw size. The leakage flaw is conservatively selected with a length equal to [ ]+. The local +a,c,e stability analysis is carried out by performing a [+a,c,e]+ of a straight piece of the RHR line pipe containing a through-wall circumferential flaw subjected to internal pressure and external loadings (faulted conditions). The objective of the local analysis is to show that unstable crack extension will not result for a flaw [ ]+ calculated by the global analysis. +a,c,e

The leak rate is calculated for the [ ]+ condition. [ ]+ +a,c,e

The crack opening area resulting from [ ]+ loads is determined from an assumed through-wall flaw of [ ]+ [ ]+ is accounted for in determining the leak rate through this crack. The leak rate is compared with the detection criterion of 1 gpm (Reg. Guide 1.45). The leak rate prediction model is an [ ]+ This method was used earlier to estimate the leak rates through postulated cracks in the PWR primary coolant loop. [1-1] +a,c,e +a,c,e +a,c,e +a,c,e

1.3 REFERENCES

1-1 Palusamy, S. S. and Hartmann, A. J., "Mechanistic Fracture Evaluation of Reactor Coolant Pipe Containing a Postulated Circumferential Through-Wall Crack", WCAP-9558 Rev. 2, Class 2, June 1981, Westinghouse Nuclear Energy Systems.

2.0 FAILURE CRITERIA FOR FLAWED PIPES

2.1 GENERAL CONSIDERATIONS

Active research is being carried out in industry and universities as well as other research organizations to establish fracture criteria for ductile materials. Criteria being investigated include those based on J integral initiation toughness, equivalent energy, crack opening displacement, crack opening stretch, crack opening angle, net-section yield, tearing modulus and void nucleation. Several of these criteria are discussed in a recent ASTM publication [2-1].

A practical approach based on the ability to obtain material properties and to make calculations using the available tools, was used in selecting the criteria for this investigation. The ultimate objective is to show that the RHR line containing a conservatively assumed circumferential through-wall flaw is stable under the worst combination of postulated faulted and operating condition loads within acceptable engineering accuracy. With this viewpoint, two mechanisms of failure, namely, local and global failure mechanisms are considered.

2.2 GLOBAL FAILURE MECHANISM

For a tough ductile material if one assumes that the material is notch insensitive then the global failure will be governed by plastic collapse. Extensive literature is available on this subject. The recent PVRC study [2-2] reviews the literature as well as data from several tests on piping components, and discusses the details of analytical methods, assumptions and methods of correlating experiments and analysis.

A schematic description of the plastic behavior and the definition of plastic load is shown in Figure 2-1. For a given geometry and loading, the plastic load is defined to be the peak load reached in a generalized load versus displacement plot and corresponds to the point of instability.

A simplified version of this criterion, namely, net section yield criterion, has been successfully used in the prediction of the load carrying capacity of pipes containing gross size through-wall flaws [2-3] and was found to correlate well with experiment. This criterion can be summarized by the following relationship:

$$Wa < Wp \qquad (2\text{-}1)$$

where Wa = applied generalized load

Wp = calculated generalized plastic load

In this report, Wp will be obtained by an [+a,c,e

]+

2.3 LOCAL FAILURE MECHANISM

The local mechanism of failure is primarily dominated by the crack tip behavior in terms of crack-tip blunting, initiation, extension and finally crack instability. The material properties and geometry of the pipe, flaw size, shape and loadings are parameters used in the evaluation of local failure.

The stability will be assumed if the crack does not initiate at all. It has been accepted that the initiation toughness measured in terms of J_{IN} from a J-integral resistance curve is a material parameter defining the crack initiation. If, for a given load, the calculated J-integral value is shown to be less than J_{IN} of the material, then the crack will not initiate.

If the initiation criterion is not met, one can calculate the tearing modulus as defined by the following relation:

$$T_{app} = \frac{dJ}{da}\frac{E}{\sigma_f^2} \qquad (2\text{-}2)$$

where T_{app} = applied tearing modulus

E = modulus of elasticity

σ_f = flow stress = [ ]$^+$ +a,c,e

a = crack length

[= +a,c,e

]$^+$

In summary, the local crack stability will be established by the two step criteria:

$$J < J_{IN}, \text{ or} \tag{2-3}$$

$$T_{app} < T_{mat}, \text{ if } J > J_{IN} \tag{2-4}$$

2.4 OPERATION AND STABILITY OF THE REACTOR RHR SYSTEM AND REACTOR COOLANT SYSTEM

The Westinghouse reactor coolant system, which for the purpose of this evaluation and report extends to the first isolation valve on the RHR lines, has an operating history which demonstrates the inherent stability characteristics of the design. This includes a low susceptibility to cracking failure from the effects of corrosion (e.g., intergranular stress corrosion cracking), water hammer, or fatigue (low and high cycle). This operating history totals over 400 reactor-years, including five plants each having 15 years of operation and 15 other plants each with over 10 years of operation.

2.4.1 Stress Corrosion Cracking

For the Westinghouse plants, there is no history of cracking failure in the reactor coolant system and connecting RHR lines. For stress corrosion cracking (SCC) to occur in piping, the following three conditions must exist simultaneously: high tensile stresses, a susceptible material, and a corrosive environment (Reference 2-4). Since some residual stresses and some degree of material susceptibility exist in any stainless steel piping, the potential for stress corrosion is minimized by proper material selection immune to SCC as well as preventing the occurrence of a corrosive environment. The material specifications consider compatibility with the system's operating environment (both internal and external) as well as other materials in the system, applicable ASME Code rules, fracture toughness, welding, fabrication, and processing.

The environments known to increase the susceptibility of austenitic stainless steel to stress corrosion are (Reference 2-4): oxygen, fluorides, chlorides, hydrozides, hydrogen peroxide, and reduced forms of sulfur (e.g., sulfides, sulfites, and thionates). Strict pipe cleaning standards prior to operation and careful control of water chemistry during plant operation are used to prevent the occurrence of a corrosive environment. Prior to being put into service, the piping is cleaned internally and externally. During flushes and preoperational testing, water chemistry is controlled in accordance with written specifications. External cleaning for Class 1 stainless steel piping includes patch tests to monitor and control chloride and fluoride levels. For preoperational flushes, influent water chemistry is controlled. Requirements on chlorides, fluorides, conductivity, and pH are included in the acceptance criteria for the piping.

During plant operation, the coolant water chemistry is monitored and maintained within very specific limits. Contaminant concentrations are kept below the thresholds known to be conducive to stress corrosion cracking with the major water chemistry control standards being included in the plant operating procedures as a condition for plant operation as well as during shutdown. For example, during normal power operation, oxygen concentration in the RCS and connecting RHR lines to the first isolation valves is expected to be less than 0.005 ppm by controlling charging flow chemistry and maintaining hydrogen at specified concentrations. Halogen concentrations are also stringently controlled maintaining chloride and fluoride concentrations within the specified limits. This is assured by controlling charging flow chemistry and specifying proper wetted surface materials.

2.4.2 Water Hammer

Overall, there is a low potential for water hammer in the RCS and connecting RHR lines since they are designed and operated to preclude the voiding condition in normally filled lines. The RC and RHR systems, including piping and components, are designed for normal, upset, emergency, and faulted condition transients. The design requirements are conservative relative to both the number of transients and their severity. Relief valve actuation and the associated hydraulic transients following valve opening are considered in the system design. Other valve and pump actuations are relatively slow transients with

no significant effect on the system dynamic loads. To ensure dynamic system stability, reactor coolant parameters are stringently controlled. Temperature during normal operation is maintained within a narrow range by control rod position; pressure is controlled by pressurizer heaters and pressurizer spray lso within a narrow range for steady-state conditions. The flow characteristics of the system remain constant during a fuel cycle because the only governing paramters, namely system resistance and the reactor coolant pump characteristics, are controlled in the design process. Additionally, Westinghouse Electric Corporation has instrumented typical reactor coolant systems to verify the flow and vibration characteristics of the system and connected RHR lines. Preoperational testing and operating experience have verified the Westinghouse approach. The operating transients of the RCS and RHRS are such that no significant water hammer can occur.

2.4.3 Low cycle and High Cycle Fatigue

Low cycle fatigue considerations are accounted for in the design of the piping system through the fatigue usage factor evaluation to show compliance with the rules of Section III of the ASME Code. A further evaluation of the low cycle fatigue loadings was carried out as part of this study in the form of a fatigue crack growth analysis, as discussed in Section 8.

High cycle fatigue loads in the RHR system would result primarily from RC pump vibrations during operation. During operation, an alarm signals the exceedance of the RC pump shaft vibration limits. Field measurements have been made on the reactor coolant loop piping of a number of plants during hot functional testing. Stresses in the elbow below the RC pump have been found to be very small, between 2 and 3 ksi at the highest. When translated to the connecting RHR lines, these stresses are even lower, well below the fatigue endurance limit for the RHR line material and would result in an applied stress intensity factor below the threshold for fatigue crack growth.

Test measurements indicate that hot leg excitation is very small and predominantly at 20 hz. The fundamental mode of the RHR lines for Catawba and McGuire is between 9 and 16 hz. Hence, the stresses in the RHR line due to RC pump vibrations will be negligible.

2.5 REFERENCES

2-1 J. D. Landes, et al., Editors, Elastic-Plastic Fracture, STP-668, ASTM, Philadelphia, PA 19109, November 1977.

2-2 J. C. Gerdeen, "A Critical Evaluation of Plastic Behavior Data and a Unified Definition of Plastic Loads for Pressure Components," Welding Research Council Bulletin No. 254.

2-3 Mechanical Fracture Predictions for Sensitized Stainless Steel Piping with Circumferential Cracks, EPRI-NP-192, September 1976.

2-4 NUREG-0691, "Investigation and Evaluation of Cracking Incidents in Piping in Pressurized Water Reactors," USNRC, September 1980.

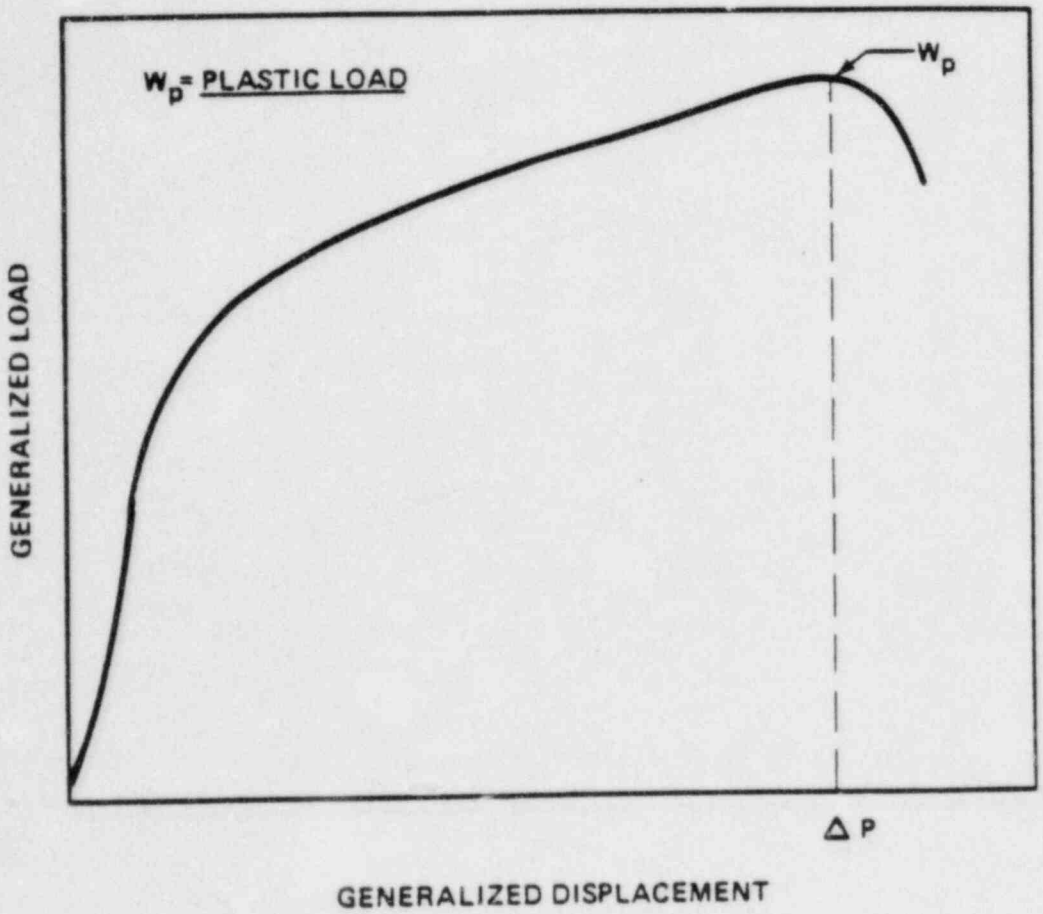

FIGURE 2-1 Schematic of Generalized Load-Deformation Behavior

3.0 LOADS FOR FRACTURE MECHANICS ANALYSIS

The RHR line stress reports [3-1, 3-2 and 3-3] were reviewed to obtain envelope loads and materials for crack stability, leak rates and fatigue crack growth evaluations. The loads were compiled from the latest computer runs identified in [3-4 and 3-5]. The envelope loads for Catawba for various applications were obtained by tabulating the applicable loads at each node of both RHR lines of the Catawba Unit 1. The same loads are applicable to Catawba Unit 2 as it is a mirror image of Unit 1. Likewise for McGuire, the applicable loads at each node of the RHR line for Unit 1 were tabulated. These loads also apply to McGuire Unit 2 as it is a mirror image of Unit 1. The portion of the RHR lines covered by this analysis is from the hot leg nozzle to the first isolation valve including all ends of the tee. Locations of the nodes are identified in Figures 3.1 and 3.2.

The stresses due to axial loads and bending moments were calculated by the following equation:

$$\sigma = \frac{F}{A} + \frac{M}{Z} \qquad (3.1)$$

where,

σ = stress
F = axial load
M = bending moment
A = metal cross-sectional area
Z = section modulus

The bending moments for the desired loading combinations were calculated by the following equation:

$$M = \sqrt{M_Y^2 + M_Z^2} \qquad (3.2)$$

where,

M = bending moment for required loading
M_Y = Y component of bending moment
M_Z = Z component of bending moment

The axial load and bending moments for various fracture mechanics applications were computed by the methods explained in Sections 3.1, 3.2 and 3.3.

3.1 CRACK STABILITY ANALYSIS

The faulted loads for the crack stability analysis were calculated by the following equations:

$$F = |F_{DW} + F_{TH1}| + |F_{SSE}| + |F_p| \quad (3.3)$$

$$M_Y = |(M_Y)_{DW} + (M_Y)_{TH1}| + |(M_Y)_{SSE}| \quad (3.4)$$

$$M_Z = |(M_Z)_{DW} + (M_Z)_{TH1}| + |(M_Z)_{SSE}| \quad (3.5)$$

where the subscripts of the above equations represent the following loading cases,

DW = deadweight
TH1 = mass thermal expansion including applicable thermal anchor motion
SSE = SSE loading including seismic anchor motion
P = load due to internal pressure

3.2 LEAK

The normal operating loads for leak rate predictions were calculated by the following equations:

$$F = |F_{DW} + F_{TH2} + F_p| \quad (3.6)$$

$$M_Y = |(M_Y)_{DW} + (M_Y)_{TH2}| \quad (3.7)$$

$$M_Z = |(M_Z)_{DW} + (M_Z)_{TH2}| \quad (3.8)$$

where the subscript TH2 represents normal operating thermal expansion loading. All other parameters and subscripts are same as those explained in Section 3.1.

3.3 FATIGUE CRACK GROWTH

The normal operating loads for fatigue crack growth analysis were computed by equations 3.6, 3.7, and 3.8, i.e., the same method as that used for leak rate loading (Section 3.2). The stresses due to normal operating loads were superimposed on through wall axial stresses due to thermal transient to obtain total stress for fatigue crack growth as explained in Section 7.6.

3.4 SUMMARY OF LOADS, GEOMETRY AND MATERIALS

Table 3-1 provides a summary of ervelope loads computed for fracture mechanics evaluations in accordance with the methods explained in Sections 3.1, 3.2 and 3.3. The cross-sectional dimensions and materials are summarized in Table 3-2.

Based on the evaluation of loads and pipe geometry, [+a,c,e] lines were identified. These locations are as follows (see Figures 3-1 and 3-2):

[+a,c,e

]

Of these locations, [+a,c,e] Both the detailed and simplified evaluations are discussed in detail in the following sections.

REFERENCES

3-1 EDS Report No. 01-0093-1155, Revision 0, "ASME Boiler and Pressure Vessel Code Section III, Class 1 Stress Report, Residual Heat Removal and Hot Leg Safety Injection Lines, Catawba Nuclear Station Unit No. 1."

3-2 Report No. SED-78-104 Revision 2, "ASME Boiler and Pressure Vessel Code Section III, Class 1 Stress Report, Residual Heat Removal System and Hot Leg Safety Injection Lines for McGuire Nuclear Station Unit No. 1."

3-3 Report No. 01-0920-1129, Revision 1, "ASME Boiler and Pressure Vessel Code Section III, Class 1 Stress Report for the Residual Heat Removal and Hot Leg Safety Injection Lines for McGuire Nuclear Station Unit No. 2.

3-4 Duke Power Letter No. CN-84M-21, February 20, 1984, "Catawba Nuclear Station Unit 1 Information Required for Fracture Mechanics Study."

3-5 Duke Power Letter No. MCN-84M-007, February 17, 1984, "McGuire Nuclear Staton Units 1 and 2 Mech. Break Evaluation - Auxiliary Line."

TABLE 3-1

CATAWBA AND MCGUIRE RHR LINE ENVELOPE LOADS(4)

a,c,e

[

]

(1) Load for Crack stability

(2) Load for Leak Rate

(3) Load for Fatigue crack growth

(4) Axial Loads include internal pressure load

Table 3-2

RHR LINE MATERIALS AND DIMENSIONS

CATAWBA

MCGUIRE

+a,c,e

[

]

(a) Reduced Thickness at Weld

(b) Nominal Thickness

(c) Per ANSI B16.9

+a,c,e

FIGURE 3-1: SCHEMATIC DIAGRAM OF CATAWBA RHR[ ] +a,c,e
SHOWING CRITICAL LOCATIONS

FIGURE 3-2: SCHEMATIC DIAGRAM OF MCGUIRE RHR [ ] +a,c,e
SHOWING CRITICAL LOCATIONS

4.0 CRITICAL FLAW SIZE CALCULATION

The conditions which lead to failure in stainless steel must be determined using plastic fracture methodology because of the large amount of deformation accompanying fracture. A conservative method for predicting the failure of ductile material is the [+a,c,e

]+ The flawed pipe is predicted to fail when the [+a,c,e

]+

This methodology has been shown to be applicable to ductile piping through a large number of experiments, and will be used here to predict the critical flaw size in the RHR line. The failure criterion has been obtained by [+a,c,e

]+ The detailed development is provided in Appendix A, for a through-wall circumferential flaw in a pipe with [+a,c,e

]+ The [ ]+ for these +a,c,e conditions is:

[ ]+a,c,e

where

+a,c,e

[ ]

[ ] +a,c,e

The analytical model described above accurately accounts for the piping internal pressure as well as imposed axial force as they affect the [+a,c,e]+ In order to validate the model, analytical predictions were compared with the experimental results [4-1] as shown in Figure 4-2. Good agreement was found.

In order to calculate the critical flaw size, a plot of the [ ]+ +a,c,e versus crack length is generated as shown in Figure 4-3. The critical flaw size corresponds to the intersection of this curve and the maximum load line.

As stated in Chapter 3, the highest stressed region for Catawba Units 1 & 2 is subjected to a faulted condition bending moment of [ ]+ and an +a,c,e axial force of [ ]+. The size of the pipe at this location is [+a,c,e] The critical flaw size at this location is [+a,c,e] for cracks smaller than +a,c,e [ ] the global stability criterion of +a,c,e Section 2.0 is satisfied. Similarly, the critical flaw size at the 6" branch side weld at the tee junction is calculated to be[ ]for Catawba +a,c,e Units 1 & 2.

For McGuire Units 1 & 2, the[ ] +a,c,e is identified as a critical region. At this location, the critical flaw size is found to be[ ] In addition, the critical flaw size for the 6" +a,c,e branch side weld at the tee junction is calculated to be[ ]for +a,c,e McGuire Units 1 & 2.

Reference

4-1 Kanninen, M. F., et al., "Mechanical Fracture Predictions for Sensitized Stainless Steel Piping with Circumferential Cracks" EPRI NP-192, September 1976.

4-2 ASME Section III, Division 1-Appendices, 1983 Edition, July 1, 1983.

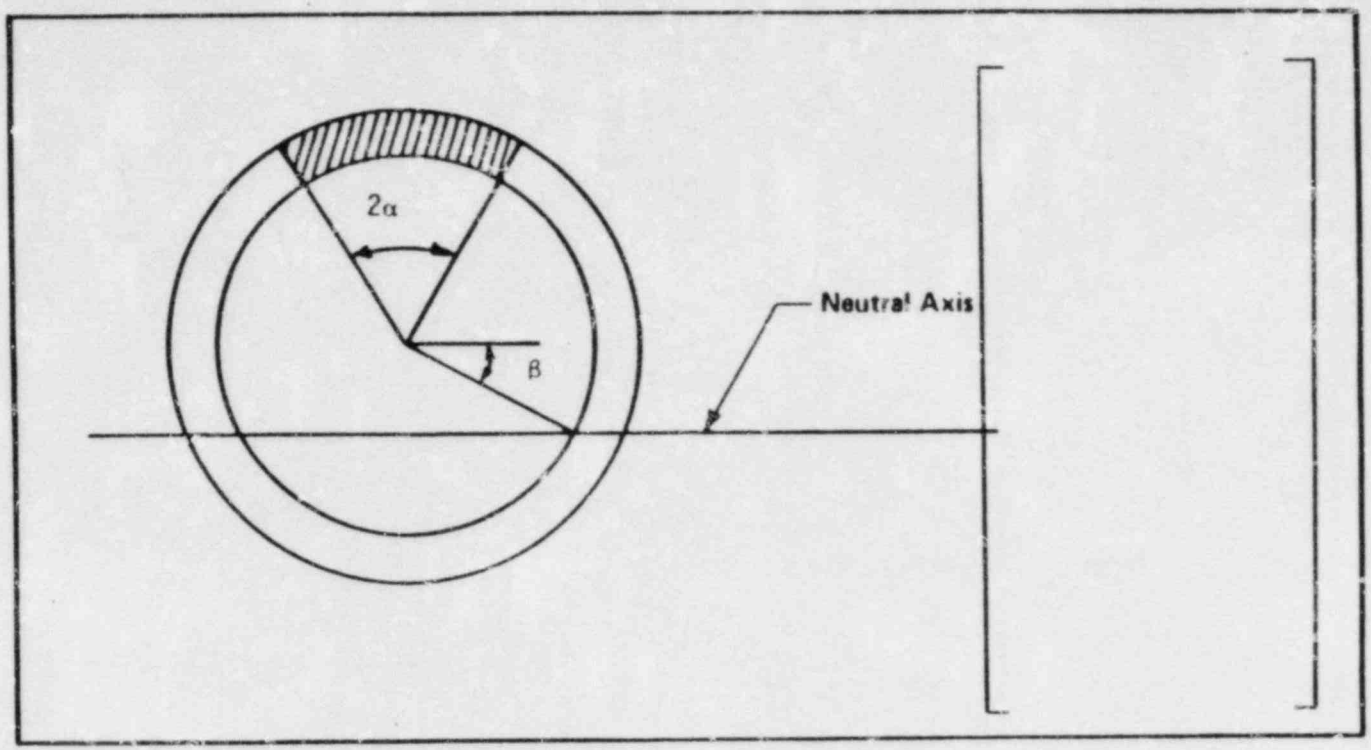

+a,c,e

FIGURE 4-1 [ ] stress distribution

+a,c,e

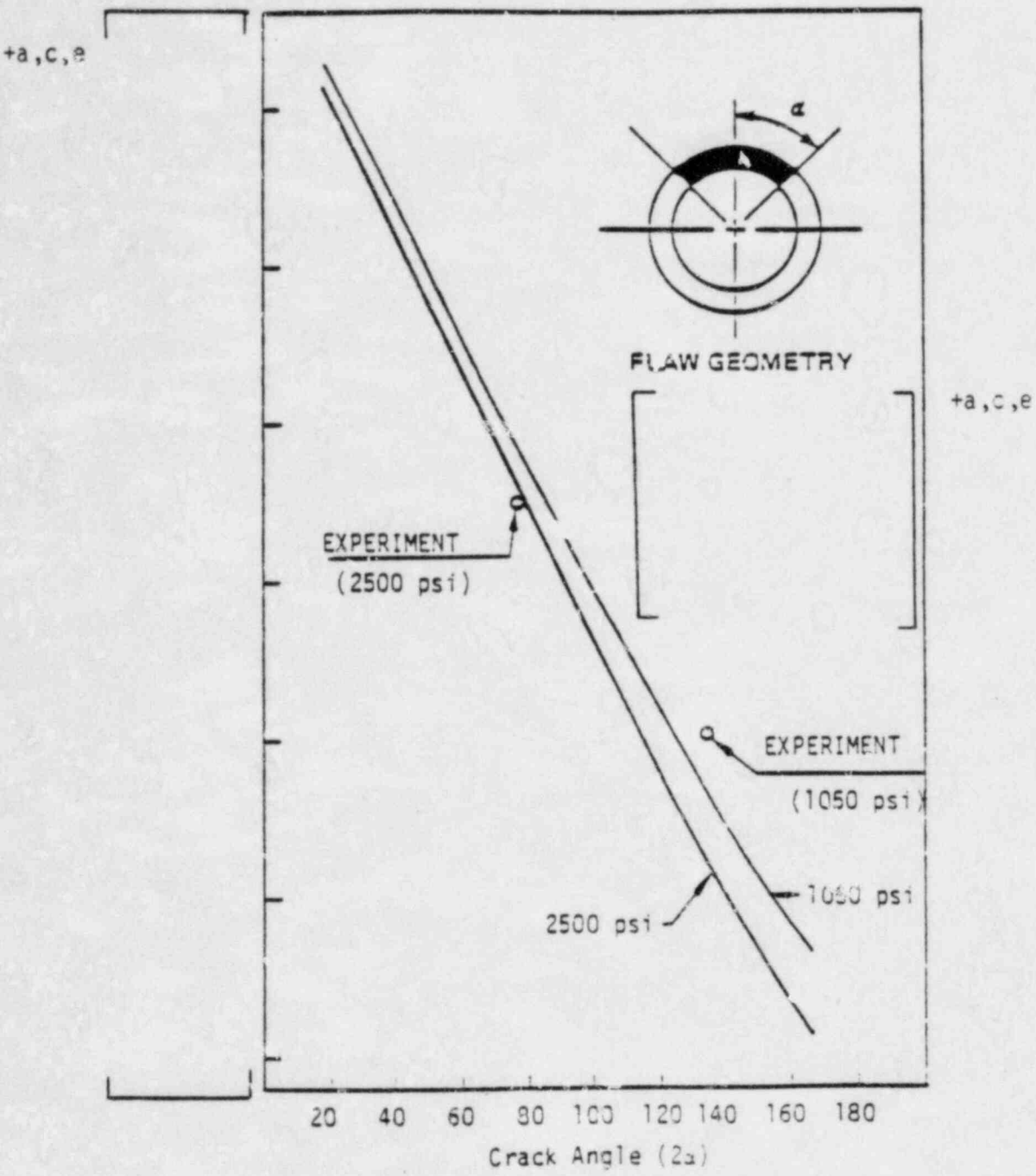

FIGURE 4-2 Comparison of[ ]predictions with Experimental +a,c,e Results

+a,c,e

FIGURE 4-3 Critical FLaw Size for RHR Line

5.0 ANALYSIS FOR CRACK STABILITY

The crack stability analyses for the RHR lines of Catawba Units 1 and 2 and McGuire Units 1 and 2 were performed for the worst locations as identified in Chapter 3 of the present report. The maximum faulted loads acting on these locations are shown in Table 5-1.

TABLE 5-1
FAULTED LOADS AND CORRESPONDING CRITICAL FLAW SIZES

+a,c,e

[

]

Based on these loads, together with an internal pressure of p = 2235 psi, the limit analyses were performed and the critical flaw sizes were determined as shown in Table 5-1. A[

]was made for the Catawba 12-inch-pipe based on a[+a,c,e

] +a,c,e

size shown in Table 5-1) to determine the local stability. The loads consist of internal pressure, external moment, and axial force including the effect of internal pressure. Simplified crack stability analyses were performed for the other 3 locations since the loads in these locations are relatively low.

5.1 THE [ ]+ MODEL AND THE MATERIAL PROPERTIES +a,c,e

Figure 5-1 identifies all the loads acting on the pipe. The pipe thickness is [ ],+ based on the thinnest location of the RHR line under +a,c,e investigation. The outer diameter is [ ]+. Due to symmetry only one +a,c,e half of the circumference, i.e., 180-degree, is modeled. The length of the model is [ ]+ which is sufficiently long to +a,c,e

attenuate the effect of the crack for correct boundary load input from the pipe end. Figures 5-2 through 5-7 all show the [ ] used for analysis. The [ ]+ are identified in Figure 5-2 through 5-5. The [ ]+ of interest for later leak rate predictions are shown in detail on Figure 5-6. The [ ] and their Z-coordinates required for the application of the axial loads and the bending moment are shown in Figure 5-7. +a,c,e +a,c,e +a,c,e +a,c,e

[+a,c,e

]+

The true stress-strain curve of the material is shown in Figures 5-8. The data are taken from the "Nuclear System Materials Handbook [5-2] for the stainless steel [ ]+ The stress-strain curve is +a,c,e
[ ]+ It has been +a,c,e
shown that the [ ]+ approximation gives good agreement with the +a,c,e
experimental results [5-3]. The material properties used in the present analysis are [+a,c,e

]+

5.2 BOUNDARY CONDITIONS AND METHOD OF LOADING

The boundary conditions are described in Figure 5-9. The pipe is subjected to the internal pressure of [ ]+ and an axial load of [ ] It +a,c,e
should be noted that the finite element pipe model is open ended and therefore the pressure applied to the internal surface of the model will not induce any axial stress. The axial load has to be added to the model separately, although it is mainly caused by the internal pressure. A bending moment of [ ]+ is then superposed to the pipe while the pressure and the +a,c,e
axial loads are held constant. Due to non-linear material behavior, the loads are added to the pipe [ ]+ +a,c,e

Figures 5-10, 5-11 and 5-12 show the sequence of applying the loads to the [ ]+ model of the pipe. Figure 5-10 shows [+a,c,

+a,c,e

]+ after which it is held steady. As shown in Figure 5-11, the axial load due to [+a,c,e

]+ Figure 5-12 shows application of the moment, starting at load step 3, where [+a,c,e

]

5.3 METHOD OF ANALYSIS

As mentioned in Section 2 of the present report the local instability criterion is based on the information of the [+a,c,e

]+

[+a,c,e

]+ This method has been successfully used to analyze a cracked pipe under a combined axial load and bending moment [5-5].

The [ ] method has been incorporated in the [+a,c,e

] to calculate the average [ ]+ of a crack as well as the +a,c,e

[ ] along the crack front for both [+a,c,e

] analyses. The [ ] at each load level can be computed by way +a,c,e of the [ ] solution strategy. +a,c,e

If the applied load is not high such that the plastic deformation in the crack tip only extends to a region small as compared to other dimensions of the structure such as the crack length or the ligament size, then the Linear Elastic Fracture Mechanics (LEFM) theory can be employed for fracture evaluations. In general, Irwin's plastic zone correction procedure [5-9] can improve the results. The simplified method is summarized as follows:

The stress intensity factors corresponding to tension and bending are expressed, respectively, by

$$K_t = \sigma_t \sqrt{\pi a}\, F_t(\alpha) \qquad (5\text{-}1)$$

$$K_b = \sigma_b \sqrt{\pi a}\, F_b(\alpha) \qquad (5\text{-}2)$$

where $F_t(\alpha)$ and $F_b(\alpha)$ are stress intensity calibration factors corresponding to tension and bending, respectively, α is the half-crack angle, σ_t is the remote uniform tensile stress, and σ_b is the remote fiber stress due to pure bending. Data of $F_t(\alpha)$ and $F_b(\alpha)$ are given in Reference [5-10]. The effect of the yielding near the crack tip can be incorporated by Irwin's plastic zone correction method [5-9] in which the crack length, a, in these formulas is replaced by the effective crack length, a_{eff}, defined by

$$a_{eff} = a + \frac{1}{2\pi} \frac{K^2}{\sigma_y^2} \qquad (5\text{-}3)$$

for plane stress plastic corrections. Where σ_y is the yield strength of the material and K is the total stress intensity due to combined tensile and bending loads. Repeated iterative procedures may be necessary for obtaining a_{eff}. However, a single correction is sufficient in general. Finally, J_I-value is determined by relation $J_I = K^2/E$, where E = Young's modulus.

In order to assure that the simplified method is valid, direct comparisons between the results of the simplified analyses and the[ ] +a,c were made. These comparisons were made for the Catawba 12-inch RHR line pipe (the present report) and the Catawba 14-inch surge line pipe [5-11]. Let these cases be named as the base cases. The comparisons were made at various points of the combined axial and bending stresses up to the yield stress. The ratio of the J-values based on the two different methods can be used to judge the correctness of the simplified method and provides a basis to make the necessary corrections.

It should be noted that this comparative method is meaningful only if the cases being analyzed have similar geometry and material properties to that of the base cases.

5.4 RESULTS OF THE STABILITY ANALYSIS FOR BASE METAL

5.4.1 [ ]RESULTS +a,c,e

It should be noted that [ ]+ refer to two stages +a,c,e
of a fracture process of a material. If the [+a,c,e
]+ Under this condition the [+a,c,e
]+ need not be evaluated. Figure 5-13 shows how the calculated value
of the [ ]+ increases up to the maximum operating loading at +a,c,e
[ ]+ At the maximum loading, the [ ]+ has a corresponding +a,c,e
value of [ ]+ as shown on the figure. The J-value as a +a,c,e
function of loads is shown in Table 5-2. The verification of the analysis is
shown in Appendix B. Since J_I at the maximum load is smaller than the
initiation toughness [ ] [5-3], crack +a,c,e
extension will not occur and tearing modulus T_{app}, does not have to be
evaluated to examine the stability condition. The stability condition is
fulfilled for the Catawba 12-inch RHR line pipe.

5.4.2 SIMPLIFIED ANALYSIS RESULTS

Based on the methods described above, the simplified crack stability analyses were performed for Catawba 6", and McGuire 14" and 6" pipes of the RHR lines. First, the J_I-values for these cases (Table 5-1) were computed using Equations 5-1 through 5-3 and the relation $J_I = K^2/E$. Note that 1/2 of the critical flaw size was used for these analyses. Second, these J_I-values were then adjusted by the J-ratios which were determined in the base cases as mentioned before. It should be noted that the base cases and the cases to be evaluated here by the simplified method are geometrically and materially similar. For the base cases, the semi-crack angles are[ ]degrees, the +a,c,e
R/t ratios are 5.8 and 5.1, and the materials are stainless steels at 617°F and 650°F. For the cases to be analyzed here by the simplified method, the semi-crack angles are ranging from[ ]degrees, the R/t ratios are +a,c
ranging from 4.6 to 6.1, and the materials are stainless steels at 617°F. These similarities suggest that the J_I-ratios obtained in the base cases can be used to adjust the J_I-values obtained by the LEFM theory for the cases

shown in Table 5-1 (with the crack length being 1/2 the critical flaw size shown in the table).

The maximum J_I ratio of the base cases, i.e., ratio of J_I of the finite element results to J_I of the simplified analysis results, is about 1.15 for the maximum load investigated (at $\sigma_{max} \simeq 0.9\ \sigma_y$). A factor of 1.5 was actually used to adjust the simplified analysis results reported herein to assure an ample safety margin. The adjusted J_I-values thus obtained are shown in Table 5-3.

It can be seen, based on the above analyses, that J_I-values of the postulated cracks shown in Table 5-1 (but with 1/2 the critical flaw size) are all smaller than the J_{IC} value of the material. The J-R curves for the 316 wrought stainless steel specimens corresponding to the minimum J_{IN} and T_{mat} are shown in Figures 5-14 and 5-15, respectively [5-3]. It should be noted that these specimens were all tested up to a load corresponding to a J_I of 12 in-kip/in^2.

It is therefore concluded that the postulated cracks (i.e., 1/2 critical flaw size as shown in Table 5-1) are all stable under the indicated loads.

5.5 RESULTS OF STABILITY ANALYSIS FOR THE WELD

For the most critical location in the Catawba 12-inch piping, the [ ]$^{+a,c,e}$ with a corresponding maximum bending moment of 1883 inch-kips. When these numerical values are substituted (as was done in Section 5.4), an applied stress intensity factor of [ ]$^{+a,c,e}$ results, using [ ]$^{+a,c,e}$ (Reference 5-7). The value of the applied J integral is then: [ ]$^{+a,c,e}$

or,

[ ]$^{+a,c,e}$

For the most critical location in the McGuire 14 inch piping, the [

] Substituting these numerical values (as above) an applied stress in- +a,c,e
tensity factor of[ ] The applied J integral is +a,c,e
then: +a,c,e

[ ]

or, +a,c,e

[ ]

Both of these values for $J_{applied}$ are well below the fracture toughness of stainless steel welds. The fracture toughness of stainless steel welds has been found to range from about [ ] to over [ ] in +a,c,e
recent studies. The weld J_{Ic} value of [ ] is representative +a,c,e
of the lower toughness values available for stainless steel welds used in commerical fabrication, and was published in Reference 5-8.

5.6 REFERENCES

5-1 [ ] +a,c

5-2 Nuclear System Materials Handbook, Volume I Design Data, Revision 1, 10/1/76.

5-3 Palusamy, S. S., Hartmann, A. J., "Mechanistic Fracture Evaluation of Reactor Coolant Pipe Containing a Postulated Circumferential Through Wall Crack," WCAP 9558, Revision 2, dated May 1982. W Proprietary Class 2

5-4 Parks, D. M., "The Virtual Crack Extension Method for Nonlinear Material Behavior," Computer Methods in Applied Mechanics and Engineering," Vol. 12, 1977, pp. 353-364.

5-5 Yang, C. Y. and S. S. Palusamy, "VCE Method of J Determination for a Pressurized Pipe Under Bending," J. of Pressure Vessel Technology, Trans. ASME, Vol. 105, 1983, pp. 16-22.

5-6 Tada, H.; P. C. Paris, and R. M. Gamble, "A Stability Analysis of Circumferential Cracks for Reactor Piping Systems", in Fracture Mechanics, ASTM STP 700, 1980, pp 296-313.

5-7 Palusamy, S. S., Tensile and Toughness Properties of Primary Piping Weld Metal for use in Mechanistic Fracture Evaluation, WCAP 9787, May 1981. W Proprietary Class 2

5-8 Bamford, W. H., et. al., The Effect of Thermal Aging on the Structural Integrity of Cast Stainless Steel Piping for Westinghouse Nuclear Steam Supply Systems, WCAP-10456, Westinghouse Proprietary Class 2, November 1983.

5.6 REFERENCES (cont'd)

5-9 Irwin, G. R., "Plastic Zone Near a Crack and Fracture Toughness, Proc. 7th Sagamore Conf., p. IV-63 (1960).

5-10 Tada, H., "The Effects of Shell Corrections on Stress Intensity Factors and the Crack Opening Area of a Circumferential and a Longitudinal Through-Crack in a Pipe", Section II-1, NUREG/CR-3464, September 1983.

5-11 Swamy, S. A., Yang, C. Y., Lee, Y. S., and Sane, A. D., "Technical Basis for Eliminating Pressurizer Surge Line Rupture as the Structural Design Basis for Catawba Units 1 and 2, WCAP-10487, Feb. 1984. W Proprietary Class 2

+a,c,e

TABLE 5-2 [J_I VS. THE APPLIED LOADS, CIRCUMFERENTIAL CRACK. [ ]

[ ] +a,c,e

+a,c,

[

]

TABLE 5-3

J_I-VALUE FOR THE SIMPLIFIED ANALYSIS

[ ] a,c,e

* Total crack length of the[ ] +a,c,e

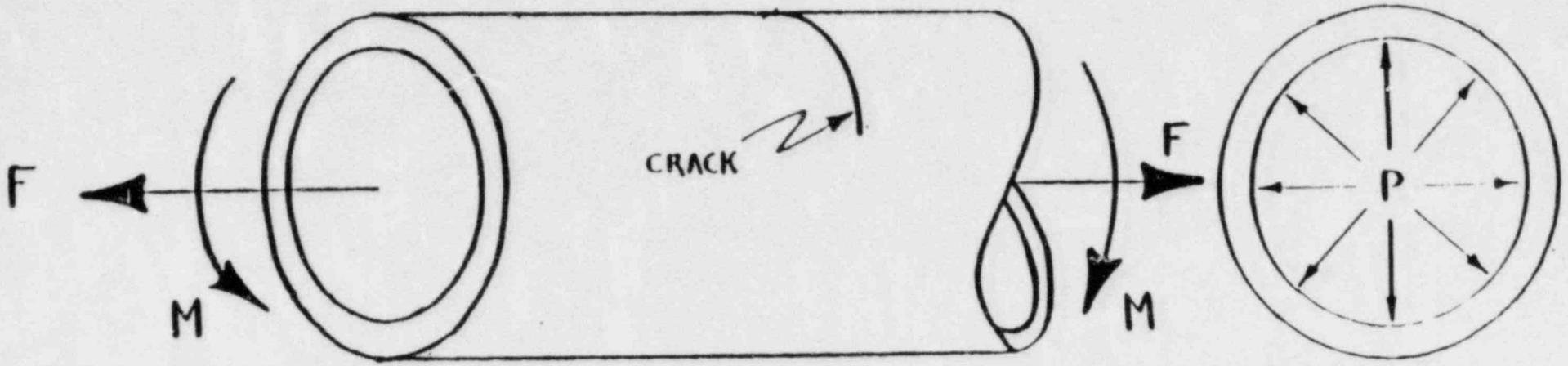

[ ] +a,c,e

FIGURE 5-1 LOADS ACTING ON THE PIPE

[ ] a,c,e

Figure 5-2 [ ] +a,c,e

+a,c,e

Figure 5-3 The [ ] model of the pipe showing [ ] +a,c,e
[ ]

+a,c,e

+a,c,e

Figure 5-4 A close-up view of the [

]

+a,c,e

Figure 5-5 The [ ]pattern in the vicinity of the crack front. +a,c,e

Figure 5-6 [ ] on the middle of the crack surface +a,c,e

+a,c,e

Figure 5-7 [ ] and their z-coordinates at the pipe end which is subjected to the +a,c,e applied axial and bending loads.

+a,c,e

Figure 5-8 [ ]Stress-Strain curve and the [ ] +a,c,e approximation.

Figure 5-9 Schematic of the boundary conditions.

+a,c,e

Figure 5-10 Loading Schedule for the internal pressure applied to the inside surface of the pipe

+a,c,e

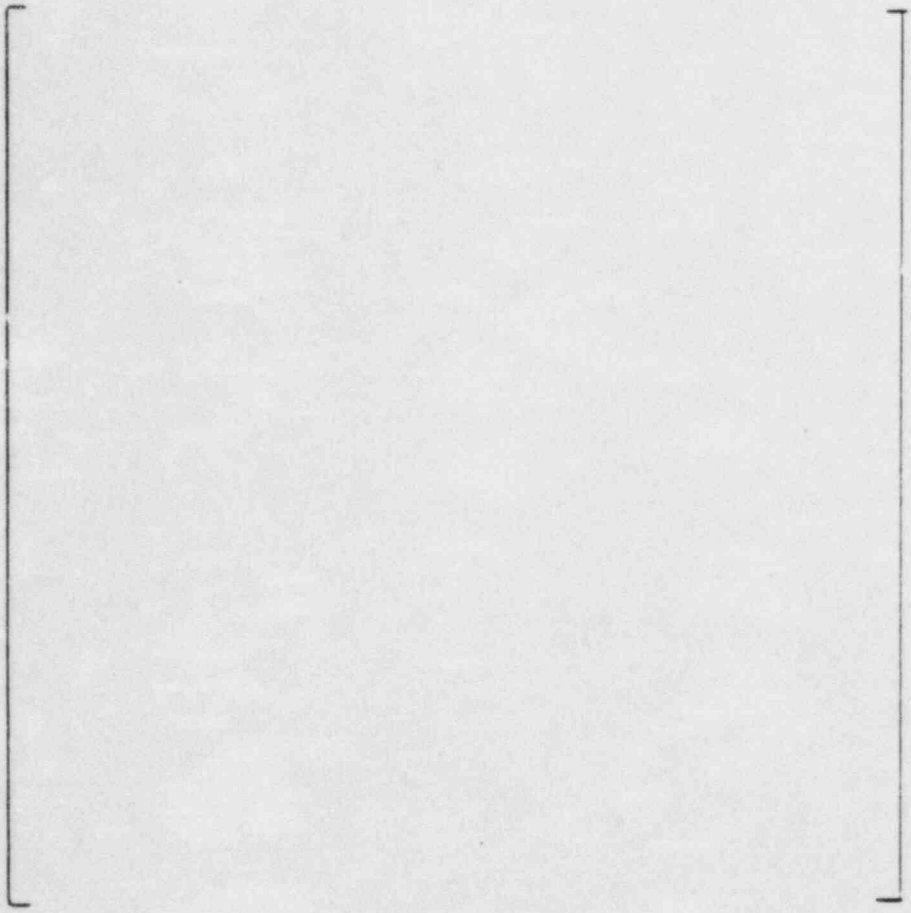

Figure 5-11 Load schedule for the uniform axial stress (including pressure) applied to the pipe end

Figure 5-12 Loading schedule for the bending moment applied to the pipe end

+a,c,e

Figure 5-13

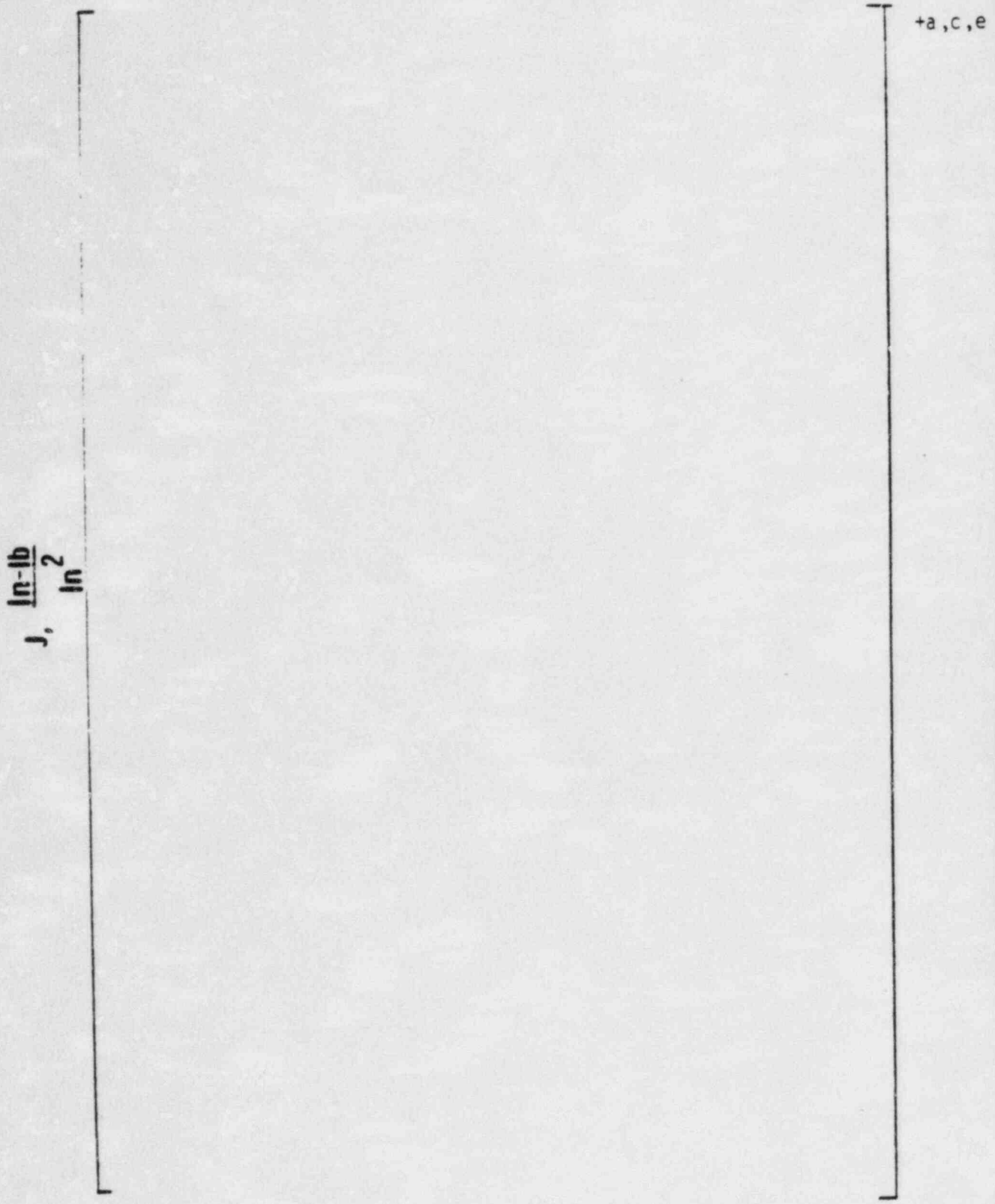

FIGURE 5-14 JR-curve for[ ]

+a,c,

+a,c,

FIGURE 5-15 JR-curve for[ ].

6.0 LEAK RATE PREDICTIONS

6.1 INTRODUCTION

The fracture mechanics analysis has shown that through-wall cracks in the RHR line would remain stable and not cause a gross failure of this RCS component. If such a through-wall crack did exist, it would be desirable to detect the leakage such that the plant could be brought to a safe shutdown condition. The purpose of this section is to discuss the method which will be used to predict the flow through such postulated cracks and present the leak rate calculation results for four locations as shown in Table 5-1. The crack lengths for these cases are[

]$^{+}$ long through wall circumferential cracks. The mechanical stability of these cracks has been shown in Section 5.0. a,c,

6.2 GENERAL CONSIDERATIONS

The flow of hot RHR water through an opening to a lower back pressure causes flashing which can result in choking. For long channels where the ratio of the channel length, L, to hydraulic diameter, D_H, (L/D_H) is greater than [ ],$^{+}$ both [ ] must be considered. In this situation the flow can be described as being single phase through the channel until the local pressure equals the saturation pressure of the fluid. At this point, the flow begins to flash and choking occurs. Pressure losses due to momentum changes will dominate for [ ] However, for large L/D_H values, friction pressure drop will become important and must be considered along with the momentum losses due to flashing. +a,c,e +a,c,e

6.3 CALCULATION METHOD

The basic method used in the leak rate calculations is the method developed by [+a,c,e

]

The flow rate through a crack was calculated in the following manner. Figure 6-1 from [ ]+ was used to estimate the critical pressure, Pc, for the RHR line enthalpy condition and an assumed flow. Once Pc was found for a given mass flow, the [ ]+ was found from Figure 6-2 of [ ] For all cases considered, since [ ]+. Therefore, this method will yield the two-phase pressure drop due to momentum effects as illustrated in Figure 6-3. Now using the assumed flow rate G, the frictional pressure drop can be calculating using +a,c,e +a,c,e +a,c,e +a,c,e

$$\Delta P_f = \left[\quad \right]^+ \qquad (6\text{-}1)$$ +a,c,

where the friction factor f is determined using the [ ]+ The crack relative roughness, ε, was obtained from fatigue crack data on stainless steel samples. The relative roughness value used in these calculations was [ ]+RMS as taken from Reference [6-3]. +a,c +a,c

The frictional pressure drop using Equation (6-1) is then calculated for the assumed flow and added to the [ ]+to obtain the total pressure drop from the primary system to the atmosphere. That is +a,c

$$\text{RHR Line Pressure} - 14.7 = [\quad]^+ \qquad (6\text{-}2)$$ +a,c

for a given assumed flow G. If the right-hand-side of Equation (6-2) does not agree with the pressure difference between the RHR line and atmosphere, then the procedure is repeated until Equation (6-2) is satisfied to within an acceptable tolerance and this then results in the flow value through the crack. This calculational procedure has been recommended by [ ]+ for this type of [ ]+calculation. The leak rates obtained by this method have been compared in Reference [ ]+ with experimental results. The comparison indicated that the method predicts leak rate with acceptable accuracy [ ].+ +a, +a, +a, +a,

6.4 CRACK OPENING AREAS AND LEAK RATES

Figure 6-4 shows the shape of one quarter of the opened crack at the mean radius of the Catawba 12"-pipe with a postulated [ ] crack, using the finite element method, when the pressure and axial loadings reach their full values of [ ], respectively. Figure 6-5 is a similar plot when a moment of [ ] is superposed upon it. Table 6-1 presents the coordinates and displacements of the [ ] used to generate the two figures. The area under each curve is evaluated by numerical integration. Multiplying each of the areas by 4 gives the total areas of the cracks at the mean radius of the pipe. The crack opening area for the other three cases, i.e. [ ] cracks, are evaluated using the simplified method [6-4]. The results of the leak rate are shown in Table 6-2. It should be noted that the L/D_h ratios for the 14" and 6" diameter McGuire piping are [ ] Therefore, the leak rates for these cases are calculated using the Henry [6-5] model for two-phase flow. The calculated leak rates for all the cases analyzed are higher than the leak detection criterion of 1 gpm (Regulatory Guide 1.45).

6.5 References

6-1[+a,c,

]

6-2[+a,c,

]

6-3 Palusamy, S. S. and Hartmann, A. J. "Mechanistic Fracture Evaluation of Reactor Coolant Pipe Containing a Postulated Circumferential Through-wall Crack," WCAP 9558 Rev. 2, Class 2, Westinghouse Nuclear Energy Systems, June 1981.

6-4 Tada, H., "The Effects of Shell Corrections on Stress Intensity Factors and the Crack Opening Area of a Circumferential and a Longitudinal Through-Crack in a Pipe", Section II-1, NUREG/CR-3464, September 1983.

6-5 Henry, R. E., "The Two-Phase Critical Discharge of Initially Saturated or Subcooled Liquid", Nuclear Science and Engineering, 41, pp. 336-342 (1970).

TABLE 6-1

CRACK SURFACE DISPLACEMENT DATA FOR THE CATAWBA
12-INCH PIPE, CRACK LENGTH [ ]a,c,e

[ ]a,c,e

TABLE 6-2

RESULTS OF LEAK RATE

a,c,

NOTES: 1, F denotes the axial load, kips

2, M denotes the bending moment, in-kips

3, COA denotes the crack opening area, in^2

+a,c,e

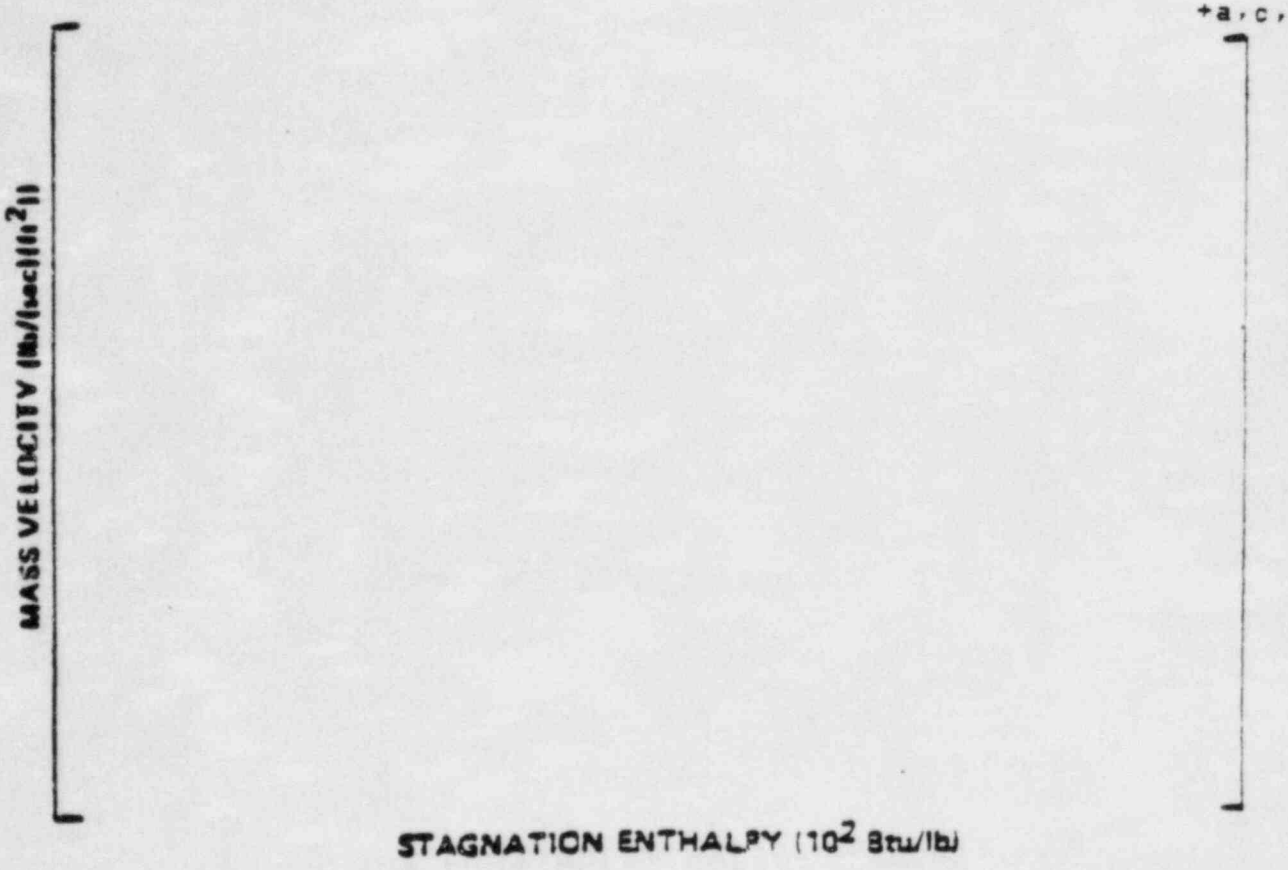

Figure 6-1 Analytical Predictions of Critical Flow Rates of Steam-Water Mixtures

+a,c

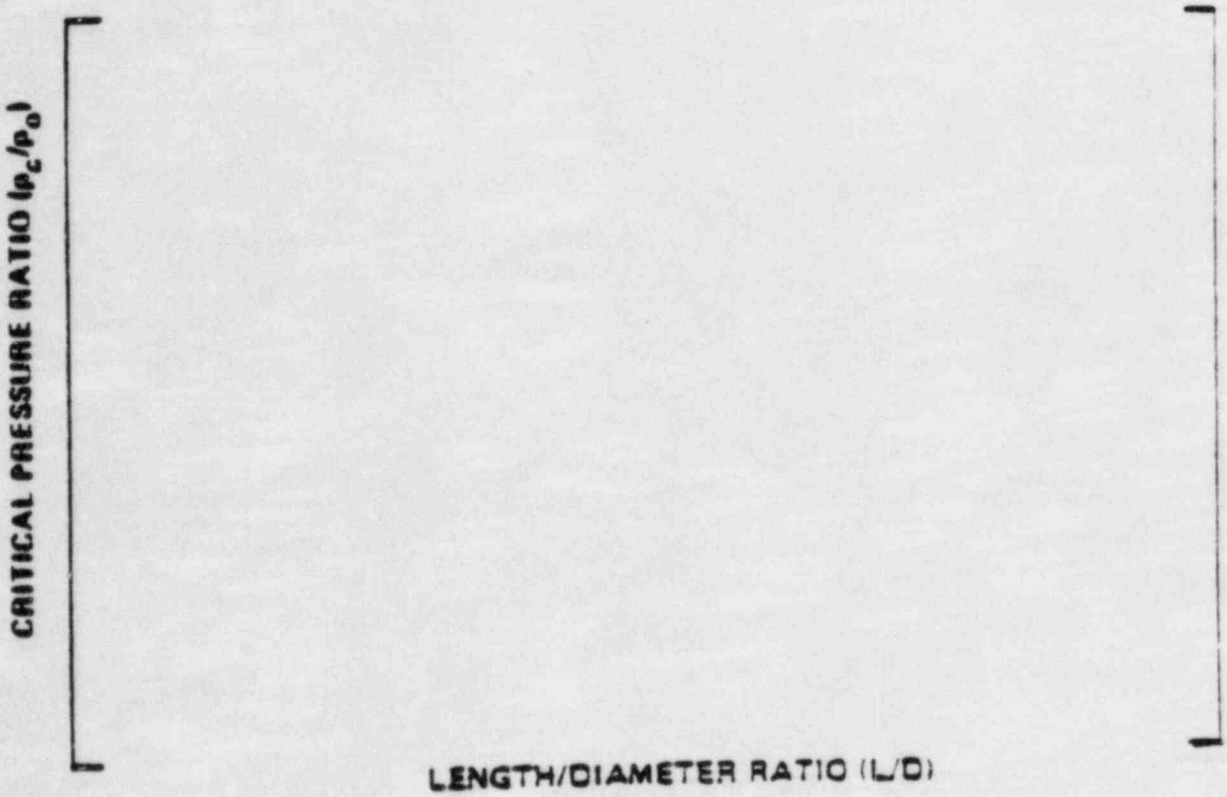

Figure 6-2 [ ] Pressure Ratio as a Function of L/D +a,c,

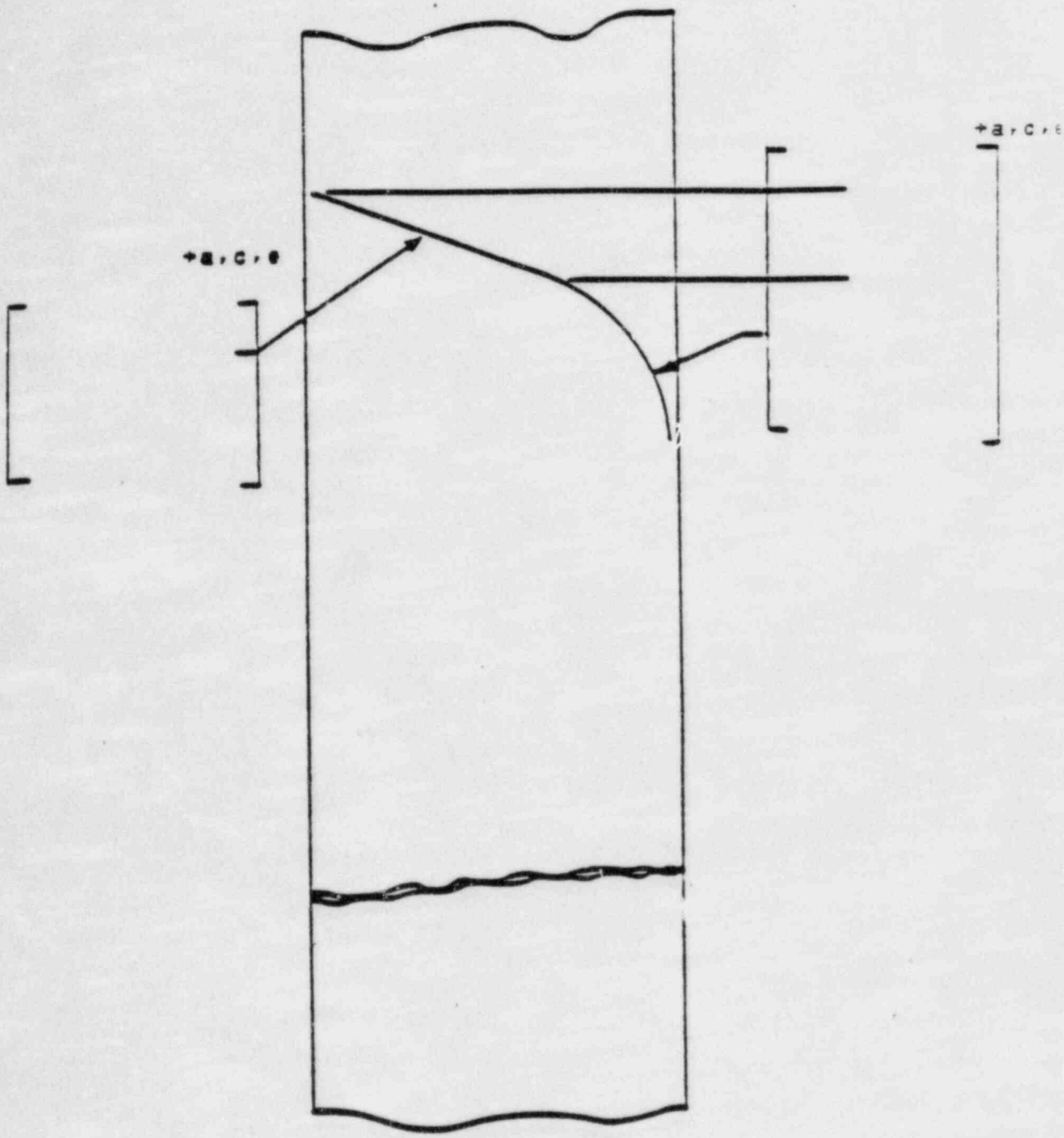

Figure 6-3 Idealized Pressure Drop Profile Through a Postulated Crack

a,c,e

+a,c,e

CRACK SURFACE DISPLACEMENT, (INCHES)

FIGURE 6-4 Crack Surface Profile under [

]

FIGURE 6-5 Crack Surface profile under combined [+a,c,e]

7.0 THERMAL TRANSIENT STRESS ANALYSIS

The thermal transient stress analysis was performed to obtain the through wall stress profiles for use in the fatigue crack growth analysis of Section 8.0. The through wall stress distribution for each transient was calculated for i) the time corresponding to the maximum inside surface stress and, ii) the time corresponding to the minimum inside surface stress. These two stress profiles are called the maximum and minimum through wall stress distribution, respectively for convenience. The constant stresses due to pressure, deadweight and thermal expansion (at normal operating temperature, [ ]) +a,c,e loadings were superimposed on the through wall cyclical stresses to obtain the total maximum and minimum stress profile for each transient. Linear through wall stress distributions were calculated by conservative simplified methods for all transients.

7.1 CRITICAL LOCATION FOR FATIGUE CRACK GROWTH ANALYSIS

The RHR line stress reports [3-1, 3-2 & 3-3, design thermal transients (Sectior 7.2), 1-D analysis of RHR line thermal transient stresses (based on ASME Section III NB3600 rules) and the geometry were reviewed to select the worst location for the fatigue crack growth analysis. The [+a,c,
] was determined to be the most critical location for the fatigue crack growth evaluation. This location is selected as the worst location based on the following considerations:

i) the fatigue usage factor is highest.

ii) the effect of discontinuity due to undercut at weld will tend to increase the cyclical thermal transient loads.

iii) the review of data shows that the 1-D thermal transient stresses in the RHR line piping secton are generally higher near the [+a,c,
]

7.2 DESIGN TRANSIENTS

The transient conditions selected for this evaluation are based on conservative estimates of the magnitude and the frequency of the temperature fluctuations resulting from various operating conditions in the plant. These are representative of the conditions which are considered to occur during plant operation. The fatigue evaluation based on these transients provides confidence that the component is appropriate for its application over the design life of the plant. All the normal operating and upset thermal transients, in accordance with design specification [7-1 and 7-2] and the applicable system design criteria document [7-3], were considered for this evaluation. Out of these, 20 transients were used in the final fatigue crack growth analysis as listed in Table 7-1.

7.3 SIMPLIFIED STRESS ANALYSIS

The simplified analysis method was used to develop conservative maximum and minimum linear through wall stress distributions due to thermal transients. In this method, a 1-D computer program was used to perform the thermal analysis to determine the through wall temperature gradients as a function of time. The inside surface stress was calculated by the following equation which is similar to the transient portion of ASME Section III NB3600, Eq. 11:

$$S_i = (A_1)\ (-\Delta T_i) + (A_2)\ (-\Delta T2_i) - A_3\ (\alpha_a TA - \alpha_b\ TB) \qquad (7.3)$$

where

S_i = inside surface stress

$$A_1 = \frac{E\alpha}{2(1 - \nu)} \qquad (7.4)$$

$$A_2 = \frac{E\alpha}{(1 - \nu)} \qquad (7.5)$$

A_3 = E_{ab} (defined in Eq. 11 of ASME NB3600) (7.6)

E = modulus of elasticity at room temperature

α = coefficient of thermal expansion at room temperature

ν = poissons ratio

α_a, α_b = coefficient of thermal expansion for pipe and nozzle section respectively

TA, TB = parameters defined in Eq. 11 of ASME NB 3600.

$\Delta T1$, $\Delta T2$ = These are calculated in 1-D thermal transient analysis. A negative value of $\Delta T1$ gives a positive tensile stress

$\Delta T2_i$ = $\Delta T2$ at inside surface.

The effect of discontinuity (3rd term of Eq. 7.3) was included in the analysis by performing separate 1-D thermal analysis for the pipe and nozzle, i.e., sections a and b, respectively. The maximum and minimum inside surface stresses were searched from the S_i values calculated for each time step of the transient solution.

The outside surface stresses corresponding to maximum and minimum inside stresses were calculated by the following equations:

$$S_{01} = (A1)\ (\Delta T1) + (A2)\ |\Delta T2_o| + (A3)|\ \alpha_a TA - \alpha_b TB| \quad (7.7)$$

$$S_{02} = (A1)\ (\Delta T1) - (A2)\ |\Delta T2_o| + (A3)|\ \alpha_a TA - \alpha_b TB| \quad (7.8)$$

where,

S_{01} = outside surface stress at time t_{max}

S_{02} = outside surface stress at time t_{min}

t_{max} = time at which S_i (eq. 7.3) is maximum

t_{min} = time at which S_i is minimum

$\Delta T2_o$ = $\Delta T2$ at outside surface

All other parameters are as defined previously

The material properties for the RHR pipe [ ] and the RCL [ ] were taken from the ASME Section III 1983 appendices [7-4] at the normal operating temperature (617°F) of the RHR line. The values of E and α, at the normal operating temperature, provide a conservative estimation of the through wall thermal transient stresses as compared to room temperature properties. The following values were conservatively used, which represent the highest of the [ ] materials.

+a,c,e

+a,c,e

+a,c,e

$$E = E_a = E_b = 25.2 \times 10^6 \text{ psi}$$
$$\alpha = \alpha_a = \alpha_b = 10.56 \times 10^{-6} \text{ in/in/°F}$$
$$\nu = 0.3$$

The maximum and minimum linear through wall stress distribution for each thermal transient was obtained by joining the corresponding inside and outside surface stresses by a straight line. The analysis discussed in this section was performed for all thermal transients of Table 7-1 for both the 12" Catawba RHR line and the 14" McGuire RHR line. The inside and outside surface stresses calculated for all transients are shown in Tables 7-2 and 7-3 for Catawba and McGuire, respectively. A schematic diagram of the RHR line geometry at the hot leg nozzle is shown in Figure 7-1.

7.4 OBE LOADS

The stresses due to OBE loads were neglected in the fatigue crack growth analysis since these loads are not expected to contribute significantly to crack growth due to small number of cycles.

7.5 TOTAL STRESS FOR FATIGUE CRACK GROWTH

The total through wall stress at a section was obtained by superimposing the pressure load stresses and the stresses due to deadweight and thermal expansion (normal operating case) on the thermal transient stresses of Table 7-2. Thus, the total stress for fatigue crack growth at any point is given by the following equation:

Total for Fatigue Crack Growth	=	Thermal Transient	+	Stress Due to DW + Thermal Expansion	+	Stress Due to Internal Pressure	(7.9)

The envelope thermal expansion, deadweight and pressure stresses, used in Equation (7.9) for calculating the total stresses, are summarized in Table 3-1 of Section 3.4.

7.6 REFERENCES

7-1 Duke Power Company Specification No. CNS-1206.02-01-000, Rev. 11, 11/22/1983, "Catawba Nuclear Station Units 1 & 2, Design Specification ASME Section III Class 1 Piping."

7-2 Duke Power Company Specification No. PSD-73-101 Rev. 2, September 1976, "McGuire Station Design Transient Analysis Class 1 Piping".

7-3 Westinghouse System Standard Design Criteria 1.3, "Nuclear Steam Supply System Design Transients," Revision 2, April 15, 1974.

7-4 ASME Section III, Division 1-Appendices, 1983 Edition, July 1, 1983.

7-5 Duke Drawing No. CN-1676-1 Rev. 3, Piping Layout Welding End Preparations.

7-6 Southwest Fabricating and Welding Co. Drawing, "ASME Section III Class 1 Butt Welding Nozzles, Rev. 3."

TABLE 7-1

THERMAL TRANSIENTS CONSIDERED FOR FATIGUE CRACK GROWTH EVALUATION

TRANS. NO.	DESCRIPTION	NO. OF OCCURRENCES
[		] a,c,e

TABLE 7-2

TRANSIENT STRESSES FOR CATAWBA RHR LINE

(psi)

+a,c,e

[

]

TABLE 7-3

TRANSIENT STRESSES FOR MCGUIRE RHR LINE

(psi)

+a,c,e

+a,c,e

+a,c,e

RHR PIPE

FIGURE 7-1: SCHEMATIC OF RHR LINE AT [ ] FOR CATAWBA/MCGUIRE

a,c,e

8.0 FATIGUE CRACK GROWTH ANALYSIS

The fatigue crack growth analyses for Catawba and McGuire Units 1 and 2 were performed to determine the effect of the transients under normal and upset conditions. They are given in Table 7-1. The analyses were performed for the critical cross section of the models which are identified in Fig. 7-1 for both Catawba and McGuire Units 1 and 2, respectively. A range of crack depths was postulated, and each was subjected to the transients in Table 7-1.

8.1 ANALYSIS PROCEDURE

The fatigue crack growth analyses presented herein were conducted in the same manner as suggested by Section XI, Appendix A of the ASME Boiler and Pressure Vessel Code. The analysis procedure involves assuming an initial flaw exists at some point and predicting the growth of that flaw due to an imposed series of stress transients. The growth of a crack per loading cycle is dependent on the range of applied stress intensity factor K_I, by the following relation:

$$\frac{da}{dN} = C_o \Delta K_I^{\,n} \qquad (8\text{-}1)$$

where "Co" and the exponent "n" are material properties, and ΔK_I is defined as ($\Delta K_I = K_{max} - K_{min}$). For inert environments these material properties are constants, but for some water environments they are dependent on the level of mean stress present during the cycle. This can be accounted for by adjusting the value of "Co" and "n" by a function of the ratio of minimum and maximum stress for any given transient, as will be discussed later. Fatigue crack growth properties of stainless steel in a pressurized water environment have been used in the analysis.

The input required for a fatigue crack growth analysis is basically the information necessary to calculate the parameter ΔK_I, which depends on the crack and structure geometry and the range of applied stresses in the area where the crack exists. Once ΔK_I is calculated, the growth due to that particular cycle can be calculated by Equation (8-1). This increment of growth is then added to the original crack size, the ΔK_I adjusted, and the analysis proceeds to the next transient. The procedure is continued in this manner until all the transients have been analyzed.

The applied stresses at the flaw location are resolved into membrane and bending stresses with respect to the wall thickness. Pressure, thermal, and discontinuity stresses are considered in the determination of the K_I factors.

The stress intensity factor at the point of maximum depth is calculated from the membrane and bending stresses using the following equation taken from the ASME Code [8-1]:

$$K_I = \sqrt{\frac{\pi a}{Q}} \left[\sigma_m M_m + \sigma_b M_b\right] \qquad (8\text{-}2)$$

where σ_m, σ_b = Membrane and bending stress, respectively

a = Minor semi-axis (flaw depth)

Q = Flaw shape parameter including a plastic zone correction factor for plane strain conditions.

$$Q = \left[\phi_1^2 - 0.212\,(\sigma/\sigma_{ys})^2\right]$$

$$\phi_1 = \int_0^{\pi/2} \left[1 - \left(\frac{b^2 - a^2}{b^2}\right) \cos^2\phi\right]^{1/2} d\phi$$

σ_{ys} = Yield strength of the material

$\sigma = \sigma_m + \sigma_b$

b = Major semi-axis (flaw length/2)

ϕ = Parametric angle of the ellipse

M_m = Correction factor for membrane stresses

M_b = Correction factor for bending stresses

The range of stress intensity factor (ΔK_I) for fluctuations of applied stress is determined by: first, finding the maximum stress intensity factor (K_{max}) during a given transient; second, finding the minimum stress intensity factor (K_{min}) during a given transient; and third, ($\Delta K_I = K_{max} - K_{min}$). At times K_{min} may go below zero; in these cases K_{min} is set equal to zero before ΔK_I is determined.

Calculation of the fatigue crack growth for each cycle was then carried out using the reference fatigue crack growth rate law determined from consideration of the available data for stainless steel in a pressurized water environment. This law allows for the effect of mean stress or R ratio ($K_{I\ min}/K_{I\ max}$) on the growth rates.

The reference crack growth law for stainless steel in a pressurized water environment was taken from a collection of data [8-2] since no code curve is available, and it is defined by the following equation:

$$\frac{da}{dN} = (0.0054 \times 10^{-3})\ (K_{eff})^{4.48} \qquad (8\text{-}3)$$

where $K_{eff} = (K_{Imax})\ (1\text{-}R)^{1/2}$

$$R = \frac{K_{Imin}}{K_{Imax}}$$

$\frac{da}{dN}$ = crack growth rate in micro-inches/cycle

8.2 RESULTS

Fatigue crack growth analyses have been performed for a range of postulated flaw sizes oriented circumferentially at the critical cross section from both Catawba and McGuire Units 1 and 2 and the results are presented in Tables 8-1 and 8-2, respectively. Postulated flaws are assumed to be six times as long as they are deep. Even for the largest postulated flaw of [

]^{a,c,e} the results show that flaw growth through the wall will not occur during 40 years design life of the plant. For smaller flaws, the flaw growths are significantly lower. For example, a postulated [ ]^{a,c,e} in deep flaw for both Catawba and McGuire Units 1 and 2 will grow to less than 1 mil. These results also confirm operating plant experience.

TABLE 8-1

FATIGUE CRACK GROWTH RESULTS
(Catawba Units 1 and 2, 12" pipe)

+a,c,

Sectio, Thickness [ ]*

a,c,e

*This is conservatively taken as minimum thickness of the counter bore region

TABLE 8-2

FATIGUE CRACK GROWTH RESULTS

(McGuire Units 1 and 2, 14" pipe)

+a,c,e

Section Thickness [ ]*

a,c,e

*This is conservatively taken as minimum thickness of the counter-bore region

TABLE 8-2

FATIGUE CRACK GROWTH RESULTS

(McGuire Units 1 and 2, 14" pipe)

+a,c,

Section Thickness [ ]*

[

a,c,e

]

*This is conservatively taken as minimum thickness of the counter-bore region

9.0 SUMMARY AND CONCLUSIONS

A mechanistic fracture evaluation of the RHR lines in the Catawba and McGuire Unit 1 and Unit 2 plants was performed. Limiting regions were identified in both the McGuire and Catawba RHR piping systems. The most limiting region to cover all RHR lines was found to be at the[+a,c,e

] evaluations were performed at this location. Simplified analytical +a,c,e methods were used for the evaluation of other limiting locations.

Corrosion, high and low cycle fatigue and water hammer were evaluated and shown either not to exist or not to cause excessive crack growth or leakage of the pressure boundary.

Thru-wall flaws were postulated to exist in both base (wrought) and weld regions of the stainless steel RHR lines.

Postulated thru-wall, circumferentially oriented flaws of[ ] +a,c,e flaw sizes as determined by[ ]were chosen as reference flaws for +a,c,e leak rate estimates. The reference flaw was [ ] inches long at the most +a,c,e limiting location. [ ]+ analysis was used to +a,c,e evaluate flaw stability by calculation of the [ ]+. The applied +a,c,e [ ] was calculated corresponding to the maximum +a,c,e applied load including the Safe Shutdown Earthquake load. The applied [+a,c,e] is thus less than [ ]+ for the wrought +a,c,e material. These results demonstrate that a [ ] crack will remain +a,c,e stable when subjected to maximum loading conditions considering both global and local failure mechanisms. The applied [ ] values at other +a,c,e limiting locations were found to be significantly lower.

Stability calculations were performed for postulated reference flaws in weld material. For the most limiting location with a postulated through-wall flaw [ ]+ inches long, the calculated [ ] is +a,c,e less than the lower bound [ ] value for the weld material [+a,c,e].

The leak rate for the reference flaw in the 12 inch pipe under normal operating loads was determined to be [ ]+a,c,e. The 6-inch pipe yielded a leak rate of [ ]+a,c,e for Catawba Units 1 & 2. These calculated leak rates are significantly greater than the leak detection criterion of 1 gpm in Regulatory GUide 1.45. For Catawba and McGuire RHR piping (12" and 14" nominal diameter) there is a margin [ ]+a,c,e relative to the leak detection criterion of (1 gpm) Regulatory Guide 1.45.

Based on the above, it is concluded that large breaks in the RHR lines should not be considered as a part of the structural design basis for Catawba Units 1 & 2 and McGuire Units 1 & 2.

APPENDIX A

EQUILIBRIUM OF THE SECTION

a,c,e

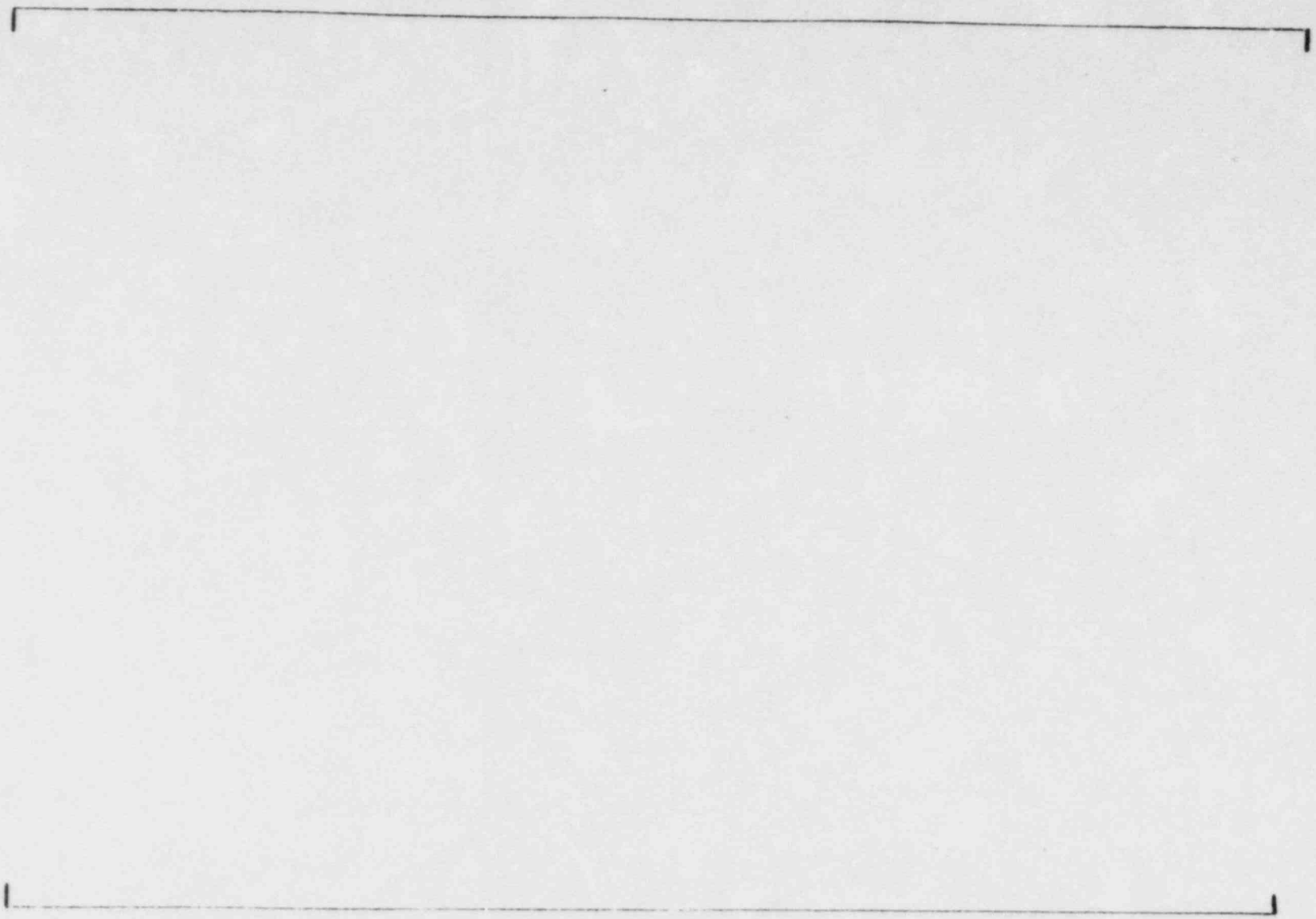

FIGURE A.1 PIPE WITH A THROUGH WALL CRACK IN BENDING

APPENDIX B

VERIFICATION OF THE[ ]RESULTS a,c,e

The purpose of the verification presented herein is to assure the correctness of the fracture mechanics analysis for the pipe. Both the K_I values due to the pure axial stretching and the pure bending are investigated. The outer fiber stresses corresponding to the maximum applied bending moment are investigated also.

(1) <u>The K_I for a circumferentially cracked pipe subjected to a uniform tensile load</u>

The elastic solution for this problem has been studied by Folias [B-1] and others. Under the present geometrical and loading conditions, the K_I is given by

+a,c,

[

]

+a,c,

[ ]+a,c,

Substituting [ ]+a,c, ksi√in. The difference between the results by Eq. (B-3) and the VCE method is 0.6 percent.

(2) K_I due to pure bending

The K_I for a circumferentially cracked pipe subjected to bending may be estimated by taking the average of that produced by the tensile outer fiber stress, σ_b, and by the fiber stress at the location of the crack tip, σ'. These stresses are shown in Figure B-1. The relation between σ_b and σ' is given by

$$\sigma' = \sigma_b \cos \alpha \qquad (B-5)$$

where α=crack angle (see Figure B-1). Therefore the K_I due to bending is

$$K_{I,b} = [\quad]^{+a,c,e} \qquad (B-6)$$

Inserting Eq. B-5 into Eq. B-6 and taking [ ], one obtains:

$$K_{I,b} = [\quad] \qquad (B-7)^{+a,c}$$

+a,c

[ ]

[ ] +a,c,e

It need be noted that Eqs. B-3 and B-7 are valid only for the elastic deformation. When loads increase the linear elastic theory underestimates the [ ] The deviation is considerable when +a,c,
large plastic zone in the crack tip region is developed. However, these equations can be used for reference purpose. This means that the actual [ ] should be always greater than those given by Eqs. B-1 and +a,c,
B-6. This condition or requirement is met for the present analysis.

(3) Check on the Outer fiber stress

In addition to examining the [ ]values, the axial stress +a,c,
which directly relates to the open mode of fracture is examined herein. Only the outer fiber stress on the tension side is checked. Since there is no plastic deformation in the region remote from the crack up to [ ]in-kip, the bending stress below this load level can be computed by +a,c

$$\sigma_b = \frac{M}{I} z \qquad (B-8)$$

where M = bending moment
I = moment of initia
z = distance from the neutral axis.

Based on the geometrical data employed in the present analysis, [+a,c,
]. For [ ] in-kip (which is the bending moment +a,c,
corresponding to load [

] In addition to +a,c

...ne bending stress, there is an axial stress, σ_a, of [ ] ksi +a,c constantly acting on the pipe. Therefore, the combined fiber stress at the Guassian point investigated is

$$\sigma_{tot} = \sigma_a + \sigma_b$$

$$= [\quad] \quad +a,c,$$

The corresponding stress given by [ ] is [ ] ksi. The error is +a,c 0.05 percent.

Reference

B-1 Folias, E. S., "On the Effect of Initial Curvature on Cracked Flat Sheets," Int. J. of Frac. Mech., Vol. 5, 1969, pp. 327-346.

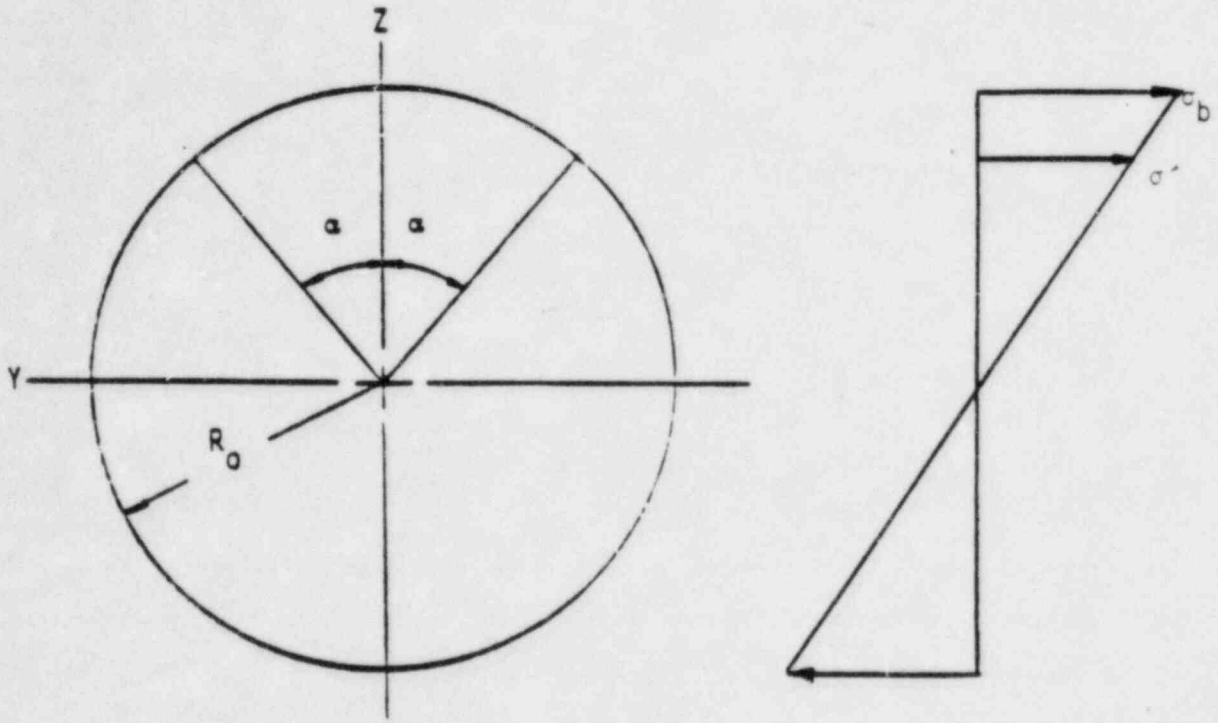

$$\sigma_b = \frac{M}{I} R_o$$

$$\sigma' = \frac{M}{I} (R_o \cos\alpha) = \sigma_b \cos\alpha$$

α = crack angle

Figure B-1 Auxiliary diagram for derivation of Equation B-6.